^{14}N overtone NMR under MAS: signal enhancement using cross-polarization methods

*Maria Concistré[1], Ilya Kuprov[1], Ibraheem M. Haies[2], Philip T.F. Williams[3], and Marina Carravetta[1]**

[1]*School of Chemistry, University of Southampton, Highfield Campus, Southampton, SO17 1BJ, UK*

[2]*University of Mosul, College of Science, Department of Chemistry*

[3]*Centre for Biological Sciences, University of Southampton, Southampton, SO17 1BJ, United Kingdom.*

Abstract

Polarization transfer methods are widely adopted for the purpose of correlating different nuclear species as well as to achieve signal enhancement. Polarization transfer from ^{1}H to the ^{14}N overtone transition (Δm=2) can be achieved using cross polarization methods under magic-angle spinning conditions, where spin locks of the order of several milliseconds can be obtained on common bio-solids (α-glycine and N-acetyl-valine). Signal enhancement factors up to 4.4 per scan, can be achieved under favorable conditions, despite MHz-sized quadrupolar interaction. Moreover, we present a detailed theoretical treatment and accurate numerical simulations which are in excellent agreement the unusual experimental matching conditions observed for cross-polarization to ^{14}N overtone.

Keywords: overtone NMR, quadrupolar NMR, cross-polarisation

1. Introduction

The supernova responsible for the isotope composition of the Earth[1] could have done a better job on nitrogen. Both isotopes are NMR active (^{14}N 99.63%, spin 1; ^{15}N 0.37%, spin 1/2), but ^{15}N is scarce and ^{14}N is hard to use – its quadrupolar interaction is typically in the MHz[2-5] range. As a result, ^{14}N NMR signals in liquids are wider than the chemical shift range, and in solids they are wider than the excitation bandwidth of radiofrequency pulses. ^{14}N NMR is considered difficult and demanding.

Currently, most NMR users favour expensive ^{15}N enriched substances, but a significant minority never gave up on ^{14}N and significant progress has been made in the solid-state: its quadrupole moment interacts with local electric fields and provides structural and dynamic information that would not otherwise be available [5-7]. Even the resolution

problem is gradually being overcome: the NMR signal of the double-quantum ("overtone", OT) transition between the outer Zeeman levels of the ^{14}N spin is orders of magnitude sharper than the single-quantum transition signal [8-15].

The OT transition is sharp because the orientation-dependent term in the transition frequency between the outer Zeeman levels of ^{14}N only depends on ω_Q^2/ω_Z, which is much smaller than ω_Q that appears in the orientation dependence of the single-quantum frequency[14, 16]. However, the downside is that the OT transition is normally forbidden. The quadrupolar interaction makes these transitions weakly allowed, but the OT transition moment is a factor of ω_Q/ω_Z smaller than that of the single-quantum transition, therefore it suffers from low sensitivity[14, 16]. Progress has also been hindered due to the absence of convenient tools to simulate OT NMR spectra as the absence of a convenient rotating frame has made numerical modelling challenging. [9]

To overcome the sensitivity problem, both polarisation transfer and hyperpolarisation have been attempted[13, 17]. In 2014, Rossini and co-workers[13] reported the first ^{14}N OT signal enhancement under MAS using ramped amplitude cross-polarization (CP) with dynamic nuclear polarization (DNP). A signal enhancement by a factor of 82 was obtained, but a long recycle delay (40 seconds) had to be used due to the long ^{1}H relaxation time at low temperature. It was also unclear how much of an effect the CP stage had – it is possible that the sensitivity gain was solely due to DNP. The acquisition conditions in those experiments were typical for CP to nuclei with large quadrupole interaction – the spin-lock condition cannot normally be fulfilled for more than few hundred microseconds[18-20].

Encouraged by these results, we performed a detailed investigation of the efficiency of a number of possible OT CP pulse sequences. Here we report a detailed theoretical and experimental analysis of the OT equivalent of the Hartman-Hahn matching conditions[21-22] for α-glycine and N-acetylvaline.

2. Materials and methods

N-acetylvaline (NAV, C_Q = 3.21 MHz) and α-glycine (Gly, C_Q = 1.18 MHz) were purchased from Sigma-Aldrich. NMR experiments were performed on a Agilent DD2 spectrometer operating at 14.09 T equipped with a 3.2 mm {^{1}H,^{13}C,^{15}N}triple resonance probe set up in double-resonance mode on ^{1}H and ^{14}N OT, a Bruker Avance II spectrometer at 19.96 T equipped with a 1.3 mm probe at the UK National Facility in Warwick.

Three CP pulse sequences were evaluated (Fig.1). The sequence in Fig. 1A is the classical constant amplitude CP[21] with decoupling on the proton channel during the acquisition. The sequence in Fig. 1B uses ramped CP where the nutation frequency on the proton channel is increased linearly from $\omega_{nut}^H - \Delta$ to $\omega_{nut}^H + \Delta$. The sequence in Fig. 1C

is an adiabatic ramp CP where the nutation frequency on the proton channel is increased from $\omega_{\mathrm{nut}}^{\mathrm{H}} - \Delta$ and $\omega_{\mathrm{nut}}^{\mathrm{H}} + \Delta$ with a tangential sweep[23] :

$$\omega_{1I}(T) - \omega_{1S}(T) - f\omega_r = b_f \tan\left[{}^{2}/_{\tau} \arctan\left({}^{\Delta}/_{b_f}\right)\left({}^{1}/_{2}\ \tau - T\right)\right]$$

$$\text{for } 0 \leq T \leq \tau$$

With only the Zeeman interaction present, the resonance frequency of the ^{14}N OT transition is 86.74 MHz at 14.09 Tesla, and 122.88 MHz at 19.96 Tesla. All OT spectra were referenced to these frequencies. The radiofrequency nutation frequency for the OT was calibrated to 55 kHz using the single-quantum ^{17}O NMR signal of liquid water, which has a similar Larmor frequency (81.4 MHz at 14.09 T).

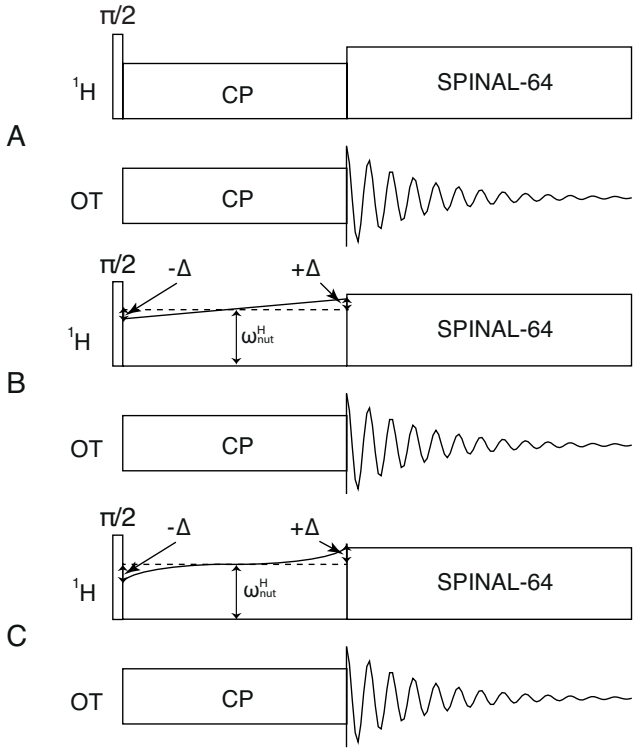

Figure 1: Overtone CP pulse sequences evaluated in this work: (A) CP with constant amplitude; (B) CP with ^{1}H amplitude ramped linearly; (C) CP with ^{1}H amplitude ramped adiabatically. The channel marked OT is tuned to twice the Larmor frequency of the ^{14}N nucleus.

The most intense signal for the ^{14}N OT transition is the second overtone sideband[9-10]. All experiments were performed on resonance with this signal. For the direct acquisition OT NMR spectra, the optimal excitation pulse duration was found to be 260 μs for both Gly and NAV. Recycle delays of 0.5 s and 0.4 s respectively were used for Gly and NAV samples and with a dead time of 70 μs. SPINAL-64 proton decoupling[24]

with $\omega_{nut}^{H}/2\pi$ = 72 kHz was applied during OT pulses and acquisition. For the CP experiments, the optimal ^{1}H nutation frequency was found to be near $\omega_{nut}^{H}/2\pi$ = 34 kHz in all cases. The CP measurements were performed using a 2.5 s recycle delay and the dead time of 1 μs at the detection stage.

3. ^{1}H-^{14}N OT Hartmann-Hahn matching conditions

In order to understand the Hartmann-Hahn matching conditions in ^{1}H-$^{14}N_{OT}$ CP schemes under MAS, a series of experiments were performed on Gly and NAV samples at different spinning speeds (20 kHz for NAV, 20 kHz and 60 kHz for Gly) and two different values of the static magnetic field (14.09 T for NAV, 14.09 T and 19.96 T for Gly). The results are shown in Fig. 2.

The most striking observation is that the OT magnetisation changes sign halfway through the matching condition. This is a known phenomenon[21], it arises when one of the two nutation frequencies in the CP experiment is so low that both the zero- and the double-quantum matching can occur. The salient point here is that the true OT nutation frequency is very low because it is proportional to the modulus of the matrix element of the perturbation operator corresponding to the radiofrequency irradiation[14, 16]

$$\omega_{nut}^{OT} = 2\gamma_N B_1 \left| \left\langle \psi_+ \right| \hat{S}_X \sin(\theta) + \hat{S}_Y \cos(\theta) \left| \psi_- \right\rangle \right| \tag{1}$$

where B_1 is the amplitude of the radiofrequency magnetic field, γ_N is the gyromagnetic ratio of ^{14}N nucleus, $\left\{\hat{S}_X, \hat{S}_Y, \hat{S}_Z\right\}$ are ^{14}N spin operators, θ is the angle that the radiofrequency coil makes with the magnetic field, and $\left|\psi_\pm\right\rangle$ are the highest and the lowest energy eigenvectors of the full ^{14}N spin Hamiltonian. Running through the second order perturbation theory and taking the powder average of the result (see the Supplementary Information) produces the following expression:

$$\left\langle \omega_{nut}^{OT} \right\rangle = \frac{1}{\sqrt{15}} \frac{\omega_1}{\omega_0} \omega_Q, \qquad \omega_Q = \frac{3e^2qQ}{2S(2S-1)} \tag{2}$$

This suggests, just as it was observed before on many occasions[9, 14, 16], that high fields are detrimental to OT spectroscopy, and large quadrupolar couplings are beneficial. High field is detrimental in the sense that the transition is more "forbidden" under those circumstances. This can be deduced from Eq. 8 in the supporting information, which also follow what previously reported by Tycko and Opella, where the probability of exciting the OT transition depends on the magnetic field.

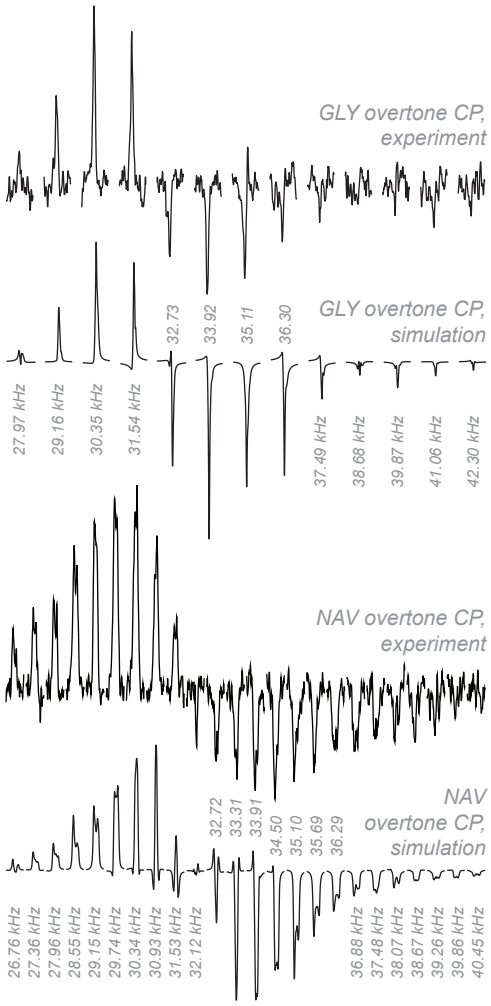

Figure 2: Experimental Hartman-Hahn matching profile acquired and simulated for the most intense OT spinning sideband of Gly (top) and NAV (bottom) using the constant amplitude CP pulse sequence in Fig. 1A with the spinning rate of 20 kHz. The contact time was 5 ms for both samples. ω_1 = 55 kHz and ω_{nut}^{H} was varied as indicated. The estimated value of ω_{nut}^{OT} is 257 Hz for Gly and 700 Hz for NAV, using Eq. 2. A total of 1024 transients were summed up to obtain the Gly spectra showed. 4000 transients in the case of NAV. Experiments are compared with numerical simulations (see text). Similar experiments were carried out for GLY at 19.96 T and spinning at 60 kHz and gave similar results (Fig. S2 in the SI).

In all experiments and simulations reported in this work $\omega_1/2\pi$ = 55 kHz. Given ω_Q = 1.18 MHz for Gly and ω_Q = 3.21 MHz for NAV, we estimate the powder averaged OT nutation frequencies at 260 Hz and 700 Hz respectively. These are very small, and so the Hartmann-Hahn matches occurring at $\omega_{\mathrm{nut}}^{\mathrm{H}} + \omega_{\mathrm{nut}}^{\mathrm{OT}} = k\omega_{\mathrm{MAS}}$ (DQ transitions, yielding positive signals in Fig. 2) and those occurring at $\omega_{\mathrm{nut}}^{\mathrm{H}} - \omega_{\mathrm{nut}}^{\mathrm{OT}} = k\omega_{\mathrm{MAS}}$ (ZQ transitions, yielding negative signals in Fig. 2) are very close to each other. This gives rise to the

experimentally observed intensity pattern. A similar behaviour was previously observed for CP between quadrupolar nuclei[25-27]. To check this qualitative interpretation, numerical simulations were performed using the Fokker-Planck module of *Spinach*[28] (described in detail in the SI) and found to be in excellent agreement with the data. It should be noted here that the CP-MAS Hamiltonian is time-independent within the Fokker-Planck formalism[29], resulting in very efficient simulations.

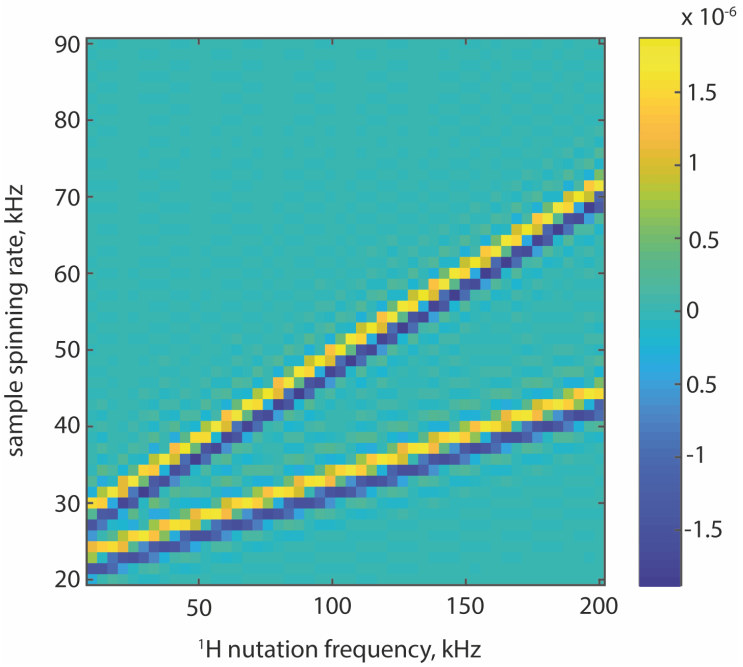

Figure 3. Simulated intensity of the second ^{14}N OT spinning sideband of Gly as a function of the spinning rate and the proton nutation frequency. The simulation was performed in *Spinach* using the parameters given in Table 1 (SI) assuming 14.09 Tesla magnet with $\omega_1/2\pi$ = 55 kHz on ^{14}N and the contact time to 0.1 ms.

Fig. 3 demonstrates that, apart from the sign switch discussed above, the Hartmann-Hahn matching conditions holds across the instrumentally accessible range of sample spinning rates and proton nutation frequencies. Given the complexity of the analytical expressions involved, additional numerical simulations were performed to confirm that the position of the Hartman-Hahn matching bands does not depend on the NQI or on the static magnetic field. The effective RF field experienced by the OT transition is very similar for both GLY and NAV and of the order of few hundred Hz in both cases. Therefore we can expect the condition for matching to be the same for both, within a similar range on the ^{1}H side. Given that the optimal CP sequence is ramped, and we have naturally some small variations of RF field along the sample volume, these small differences should be negligible

4. Ramped cross-polarisation sequences

To determine which of the three CP schemes in Fig. 1 performs best, we used all three pulsesequences for both Gly and NAV. The results are compared with the direct acquisition NMR spectrum in Fig. 4. The respective enhancement factor, calculated as the ratio between the signal area obtained in a CP experiment and that obtained in the direct OT acquisition (normalized for the number of scans), is summarized in Table 1.

The enhancement per unit scan is consistently more significant for NAV and is negligible for Gly (we get an enhancement of 1.1 by using ramped and adiabatic CP with respect to the direct acquisition). There is no significant net signal increase per unit time for either sample, given that the ^{1}H imposed pulse delay is 5 times longer than the time between pulses used for direct ^{14}N excitation. The long-time limit of the cross-polarisation enhancement is a complicated function of the spin temperature, the dipolar interaction magnitude, and the relaxation rates across the relevant transitions. Because spinning is involved, a time-independent steady-state expression is unlikely to exist. However, from qualitative considerations, we can recommend using the procedures described in this paper for systems where overtone transition relaxation is slower than both the dipolar interaction, and the proton relaxation. In all systems that we have looked at so far, this assumption appears to hold – the cross-polarisation build-up curves have a timescale characteristic of the dipolar interaction, meaning that any interfering processes are slower.

The CP schemes involving either a linear or a tangential amplitude sweep gives comparable enhancements, which are consistently better than those obtained with constant amplitude CP, with a maximum observed signal enhancement of 4.4 for NAV under optimal conditions. Experiments have also been performed using an adiabatic CP scheme with the adiabatic amplitude sweep on the ^{14}N-OT channel (spectra not shown) but this resulted in smaller signal enhancements for both samples as compared to all other CP schemes. Note also that the observed linewidth (of the order of a few kHz) is mainly due to higher order quadrupolar terms, given the fact that OT are not affected by first order quadrupolar interactions.

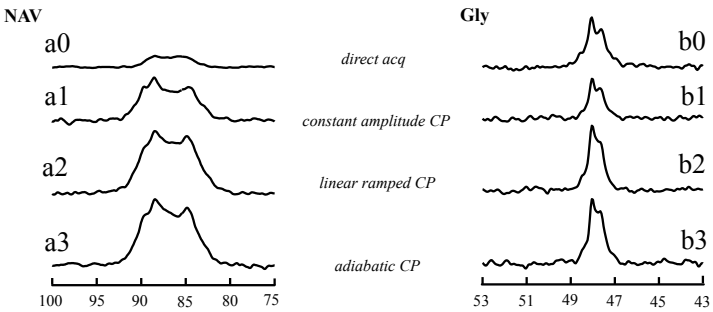

Figure 4: Comparison between experimental spectra obtained using direct acquisition and the CP pulse sequences reported in Fig. 2. The spectra on the left (a0-a3) refer to NAV, the ones on the right (b0-b3) to Gly. In all cases $\omega_r / 2\pi$ = 20 kHz, $\omega_1 / 2\pi =$ 55 kHz and $\omega_{nut}^H =$ 35 kHz was used. NAV spectra a1-a3, are the sum of 10000 transients and were collected using a 10 ms long contact time. Gly spectra b1-b3, are the sum of 1024 transients and were collected using a 5 ms long contact time. a0) Direct acquisition (90-acquire) spectrum of NAV, 160000 transients and 260 μs ^{14}N-pulse length; b0) Direct acquisition spectrum of Gly, 1024 transients and 260 μ s ^{14}N-pulse length; a1) constant amplitude CP (Fig. 2A) spectrum of NAV; b1) constant amplitude CP spectrum of Gly; a2) linearly-ramped CP (Fig. 2B) spectrum of NAV with Δ / ω_{nut}^H = 0.05; b2) linearly-ramped CP spectrum of Gly with Δ / ω_{nut}^H = 0.05; a3) adiabatic CP (Fig. 2C) spectrum of NAV with Δ / ω_{nut}^H = 0.05 and b_{cp} / ω_{nut}^H = 0.06; b3) adiabatic CP spectrum of Gly Δ / ω_{nut}^H = 0.05 and b_{cp} / ω_{nut}^H = 0.06.

The effect of introducing a ramp, linear or tangential, has been explored experimentally and results of this investigations are reported in Fig. 5.

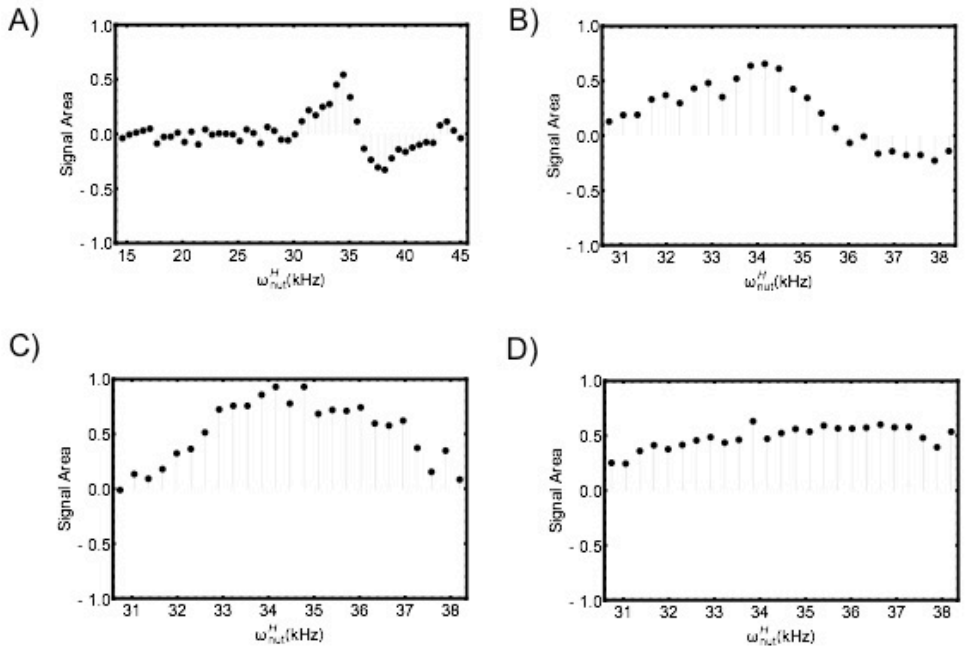

Figure 5. Experimental Hartman-Hahn matching profile acquired for Gly using a spin rate of 20 kHz, 5 ms contact time, $\omega_1 / 2\pi = 55$ kHz and $\omega_{nut}^H / 2\pi$. The estimated value of $\omega_{nut}^{OT} / 2\pi$ is 257 Hz. Signal changes are best appreciated with a signal area normalized with respect to the most efficient CP experiment. A) constant-amplitude CP pulse sequence in Fig. 2A; B) linearly ramped-CP of Fig. 2B with $\omega_{nut}^H / 2\pi = 80$ KHz and Δ = 0.1; C) linearly ramped-CP of Fig. 2B with $\omega_{nut}^H / 2\pi = 80$ kHz and Δ = 0.05; D) linearly ramped-CP of Fig. 2B with $\omega_{nut}^H / 2\pi = 80$ kHz and Δ = 0.03.

In absence of ramp we see both positive and negative transfers corresponding to the +/- HH conditions overlapping due to low effective RF on the OT (Eq. 2). As the size of the ramp increases then we have an overall increase of the experimental efficiency and the positive signal becomes dominant, cancelling out the weaker negative intensity.

To understand the role of the contact time in ^{1}H-^{14}N-OT CP, a series of experiments, on both Gly and NAV samples, that uses the linearly-ramped CP scheme of Fig. 1B have been run at different values of the contact time. The resulting signal area is normalized to the intensity of the signal obtained in a 90-acquire OT direct detection experiment (we address this ratio as the *enhancement factor*) and then plotted against the value of the contact time in Figure 6. For these experiments, we used $\omega_{nut}^{H} / 2\pi = 35$ kHz, $\omega_1 / 2\pi =$ 55 kHz, $\omega_r / 2\pi = 20$ kHz and $\Delta / \omega_{nut}^{H} = 0.05$.

The enhancement factor obtained on NAV (Figure 6, gray points) is significantly higher than that obtained for Gly (Figure 6, black points) at any value of the contact time and it reaches a plateau at about 8 ms. The enhancement factor for Gly (less than 1) reaches its maximum at about 4 ms and then slowly decrease further.

A possible explanation is that the different behaviour of the two systems and the overall lower efficiency observed in Gly is to be related to the different dynamics (due to the motion of the NH3 group) around the amide-bond of NAV and the highly mobile amine group of Gly, which interferes the polarization transfer. Moreover the optimal contact times are significantly longer than those reported in Rossini *et al.* [30] by at least one order of magnitude, and significantly longer than what typically reported for quadrupolar nuclei, where the large NQI and the difficulty at achieving an effective spin lock typically lead to very short contact times.

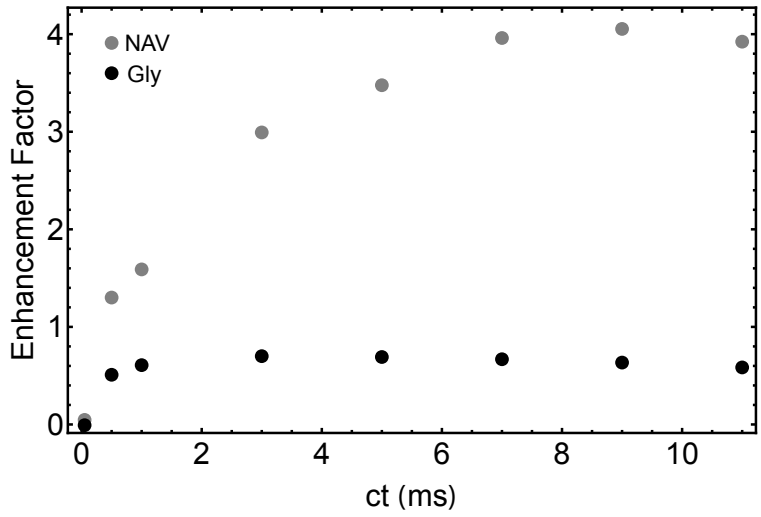

Figure 6: Experimental enhancement factors plotted against the contact time (ct) obtained as integrated area ratio between a CP and a direct excitation experiments, per unit scan. $\omega_{nut}^{H} / 2\pi = 35$ kHz, $\omega_1 / 2\pi =$ 55 kHz and $\omega_r / 2\pi$ = 20 kHz. Grey circles refer to experiments on NAV and are the sum

of 4096 acquisitions; Black circles refer to experiments on Gly and are the sum of 1024 acquisitions. In both cases a linearly-ramped CP scheme (Fig. 2B) with $\Delta / \omega_{nut}^{H}$ = 0.05 was used.

Finally, we note that the shape of the powder patterns under direct excitation and CP match well, indicating that the polarization transfer efficiency is similar for all crystallite orientations under the CP conditions used. This is a significant advantage over OT excitation via PRESTO[17] where the excitation was highly orientation dependent and only some crystallites could be effectively excited and enhanced. On the other hand, the overall efficiency obtained through CP for Gly is not as good as that reported using PRESTO, and this may be due to the fact that PRESTO requires only a few hundreds of microseconds for the transfer while CP contact time of a few milliseconds is required to build the polarization on the OT. Over this longer time, there may be signal losses for groups which are more affected by the dynamics in the system, like the amine group of Gly.

Conclusions

This works highlights the possibility of using CP for the observation of the OT transition, while faithfully preserving the peak lineshape and providing a significant signal enhancement for rigid systems.

The CP conditions we found are very robust to variations of the nature of the site and to the external magnetic field. Overtone CP is also very easy to set up, as the effective OT frequency can be expected to be below 1 kHz for a wide range of magnetic fields and NQIs, therefore a simple calibration of the proton nutation frequency to the desired value is all that is required to set up the CP at any spin rate. The ramped or adiabatic CP experiments are expected to show good performance for a wide range of spinning frequency regimes, from theoretical predictions.

Our experimental findings are supported by analytical calculations and accurate numerical simulations, which are capable of reproducing even the slightest variation in peak shape or sign, and allow to predict conditions for effective OT CP for a variety of experimental conditions.

The main drawbacks of this method are the moderately narrow-band nature of the OT excitation condition, as well as the added time to transfer polarization from the slower relaxing proton when compared to direct OT excitation and observation.

Acknowledgements

We would like to thank EPSRC (EP/M023664/1) for funding this project. The authors would like to thank J. Jarvis for useful discussions. The UK 850 MHz solid-state NMR Facility used in this research was funded by EPSRC and BBSRC, as well as the University of Warwick including via part funding through Birmingham Science City Advanced Materials Projects 1 and 2 supported by Advantage West Midlands (AWM) and the European Regional Development Fund (ERDF). We also acknowledge the use of the IRIDIS High Performance Computing Facility and associated services at the University of Southampton.

References

[1] H. B. T. Giavani, J. Skibsted and H. J. Jakobsen, *J. Magn. Reson.* **2004**, *166*, 262-272.
[2] L. A. O. Dell, *Prog. Nucl. Magn. Reson. Spectrosc.* **2011**, *59*, 295-318.
[3] R. W. Schurko, *Acc. Chem. Res.* **2013**, *46*, 1985-1995.
[4] S. Cavadini, *Prog Nucl Mag Res Sp* **2010**, *56*, 46-77.
[5] Z. H. Gan, *J. Am. Chem. Soc.* **2006**, *128*, 6040 - 6041.
[6] S. Cavadini, A. Abraham, S. Ulzega, G. Bodenhausen, *J. Am. Chem. Soc.* **2008**, *130*, 10850 - 10851.
[7] A. S. Tatton, T. N. Pham, F. G. Vogt, D. Iuga, A. J. Edwards, S. T. Brown, *CrystEngComm* **2012**, *14*, 2654 - 2659.
[8] L. A. O'Dell, R. He, J. Pandohee, *CrystEngComm* **2013**, *15*, 8657-8667.
[9] L. A. O'Dell, A. Brinkmann, *Journal of Chemical Physics* **2013**, *138*.
[10] L. A. O'Dell, C. I. Ratcliffe, *Chemical Physics Letters* **2011**, *514*, 168-173.
[11] Y. Nishiyama, M. Malon, Z. H. Gan, Y. Endo, T. Nemoto, *Journal of Magnetic Resonance* **2013**, *230*, 160-164.
[12] J. A. J. I. M. Haies, L. J. Brown, I. Kuprov, P. T. F. Willianson, M. Carravetta, *Phys. Chem. Chem. Phys* **2015**, *17*, 23748-23753.
[13] A. J. Rossini, L. Emsley, L. A. O'Dell, *Phys Chem Chem Phys* **2014**, *16*, 12890-12899.
[14] R. Tycko, S. J. Opella, *J. Chem. Phys*
1987, *86*, 1761-1774.
[15] R. Tycko, S. J. Opella, *J. Am. Chem. Soc.* **1986**, *108*, 3531-3532.
[16] L. Marinelli, S. Wi, L. Frydman, *Journal of Chemical Physics* **1999**, *110*, 3100-3112.
[17] I. M. Haies, J. A. Jarvis, H. Bentley, I. Heinmaa, I. Kuprov, P. T. W. Williamson, C. M., *Phys. Chem. Chem. Phys* **2015**, *17*, 6577-6587.
[18] A. J. Vega, *Solid State Nucl. Magn. Reson.* **1992**, *1*, 17-32.
[19] A. J. Vega, *J. Magn. Reson.* **1992**, *96*, 50.
[20] W. Sun, J. T. Stephen, L. D. Potter, Y. Wu, *J. Magn. Reson. Ser. A* **1995**, 181-188.
[21] D. Rovnyak, *Concepts in Magnetic Resonance Part A* **2008**, *32A*, 254-276.
[22] Hartmann S.R., H. E.L., *Phys Rev* **1962**, *128*, 2042-2053.

[23] S. Hediger, B. H. Meier, R. R. Ernst, *Chem. Phys. Lett.* **1995**, *240*, 449 - 456.
[24] B. M. Fung, A. K. Khitrin, K. Ermolaev, *Journal of Magnetic Resonance* **2000**, *142*, 97-101.
[25] M. A. Eastman, *J. Magn. Reson.* **1999**, *139*, 98-108.
[26] J. C. C. Chan, M. Bertmer, H. Eckert, *Chem. Phys. Lett.* **1998**, *292*, 154-160.
[27] B. H. Meier, *Chem. Phys. Lett.* **1992**, *188*, 201-207.
[28] H. J. Hogben, M. Krzystyniak, G. T. P. Charnock, P. J. Hore, I. Kuprov, *Journal of Magnetic Resonance* **2011**, *208*, 179-194.
[29] I. Kuprov, *J Magn Reson* **2016**, *270*, 124-135.
[30] A. J. Rossini, L. Emsley, L. A. O'Dell, *Phys Chem Chem Phys* **2014**, *16*, 12890-12899.